

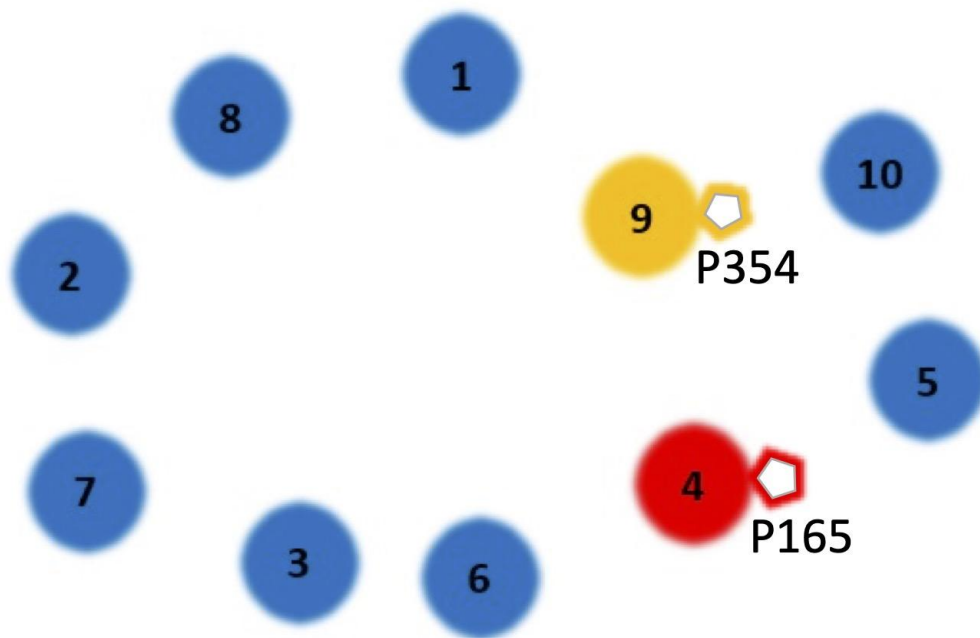
Substitution of Pro¹⁶⁵ in Transmembrane 4 of PfCRT Abolishes Lysosome Acidification Function in Stably Transfected HEK-293 Cells

Running title: Pro¹⁶⁵ in mut-PfCRT is essential for lysosome acidification of HEK-293F cells.

Keywords: Proline mutations; PfCRT; heterologous expression; lysosome-acidification; *Plasmodium falciparum*.

ABSTRACT

The *Plasmodium falciparum* chloroquine resistance transporter (PfCRT) is localised on the parasite digestive vacuole, an organelle that maintains an acidic lumen. Here we demonstrated the isolation of HEK-293F cells stably expressing wild type 3D7 and mutant *Pfcr*t alleles. Immuno-fluorescence staining of HEK-293F transfectants confirms the localization of *Pfcr*t alleles to the lysosomal vesicles. Moreover, cells expressing mut-PfCRT^{ETSE} showed greater lysosomal acidification as demonstrated by the dramatic increase in the accumulation of two weak bases, acridine orange and CytPainter LysoOrange dyes. Furthermore, HEK-293 cells stably expressing mut-PfCRT^{ETSE} with a single substitution of proline 165 in transmembrane 4 completely inhibited the accumulation of weak bases. Taken together, our results demonstrate the role of Pro¹⁶⁵ in PfCRT lysosomal acidification function in HEK-293F cells.



Schematic representation of the spatial arrangement of PfCRT TMDs based on 3D structure. In red and yellow are TMD 4 and 9, respectively. The positions of the highly conserved proline residues in TMD 4 and 9 are indicated relative to the core cavity.

Graphical Abstract

INTRODUCTION

The human malaria ~~disease~~ is a major public health problem in tropical countries with *Plasmodium falciparum* infections accounting for the majority of the total malaria cases [1]. The progression of antimalarial treatment from the natural product quinine to chloroquine (CQ) extended the effectiveness of antimalarials for nearly 20 years [2]. However, the rise of CQ resistant parasites, largely due to mutations in *Plasmodium falciparum* Chloroquine Resistant Transporter (*pfcr*t), was a major setback given the safety and efficacy of this drug [3]. Several mutant alleles of *pfcr*t have been identified in CQ-resistant field isolates [4], including the key CQ-resistance causative mutation at position 76 (Lys76Thr) of PfCRT [5]. PfCRT encodes a 424 amino acids polypeptide, with 10 transmembrane (TM) helices, localized to the digestive vacuole (DV) of the parasite [6]. A recent report, using single-particle cryo-electron microscopy, revealed the three-dimensional structure of PfCRT at a resolution of 3.2Å [7]. PfCRT structure revealed eight transmembrane helices (TMs 1-4 and 6-9) forming the central cavity of 25Å diameter with the resistance causative mutations localized to TM helices of the central cavity [8]. Transmembrane helices 4 and 10 are positioned outside the central cavity and thought to contribute to the “*open and closed*” conformations on the vacuolar side; while TMs 4 and 9 play the same role on the opposite side of the membrane in a “*rocker-switch*” motion [9]. Based on PfCRT resolved 3D structure, it was of interest to examine the effects of substituting two highly conserved proline residues (Pro¹⁶⁵ and Pro³⁵⁴) in PfCRT TMs 4 and 9 on its lysosomal acidification activity in HEK-293F cells. In this report, we show the effects of specific substitutions in mut-*pfcr*t allele on its *in-situ* lysosomal acidification function and propose that

this function of mut-PfCRT in HEK-293 cells can acts as a segregate assay for its CQ-resistance role in *P. falciparum*.

MATERIAL METHODS

Cloning of codon optimized PfCRT mutants - Wild-type *pfcrt* (3D7) encoding the CQ sensitive gene sequence obtained from plasmid DB (gene ID PF3D7_1133400) was human codon optimised and commercially synthesized (Genscript®, USA). The full-length *pfcrt* coding sequence was excised from pUC57 vector and re-ligated into pCDNA3.1+ (Invitrogen™) at restriction sites Bam-HI and Eco-RI (New England Biolabs Inc.) with a Kozak consensus sequence included. *PfCRT* allele encoding mutations shown to confer CQ resistance (mut-PfCRT^{ETSE}), as described earlier by Summers *et al.* [4]; D17 variant) was constructed by ligating 3 fragments, amplified using the Phusion High-Fidelity DNA Polymerase (Life Technologies™), possessing 4 point mutations (e.g., N75E, K76T, A220S & Q271E) into the humanised 3D7-*pfcrt* (wt-PfCRT^{NKAQ}) gene sequence using the Gibson assembly approach [10]. The latter approach was also used to introduce mutations at positions Pro165 to Ala (P165A) and Pro354 to Ala (P354A) in *D17-pfcrt* allele (or mut-P165A-PfCRT^{ETSE} and mut-P354A-PfCRT^{ETSE}). For primers sequences and reaction conditions see tables I and II (Supplementary material).

Tissue culture and selection of stable transfectants - HEK-293F cells were cultivated and maintained in DMEM culture media (Gibco™) containing 10% (v/v) fetal bovine serum (FBS) at 37°C. Cells were grown to 70-80% confluency prior to transfection. Transfections, using pCDNA3.1+ empty plasmid, full-length wt-PfCRT^{NKAQ}, mut-PfCRT^{ETSE}, mut-P165A-

PfCRT^{ETSE} and mut-P354A-PfCRT^{ETSE} containing plasmids, were linearized with MfeI restriction enzyme (New England Biolabs Inc.) and transfected into HEK-293F cells using Lipofectamine 2000 (Invitrogen™), following manufacturer's instructions. Clones from several transfections were selected in 800 µg/ml G418 in 10 % (v/v) FBS/DMEM and allowed to proliferate for several weeks prior to freezing aliquots from each clone in liquid nitrogen. Two clones for wt-PfCRT^{NKAQ} (clone 2 and 4), two clones for mut-PfCRT^{ETSE} (clones 8 and 9) and one clone for the mut-P165A-PfCRT^{ETSE} were isolated and allowed to proliferate continuously in the presence of G418 prior to characterization for PfCRT (wt or mutant) expression and drug transport studies. Unfortunately, it was not possible to obtain additional clones for mut-P165A-PfCRT^{ETSE} or any clones for mut-P354A-PfCRT^{ETSE}, after several transfection and selection attempts.

Protein extraction and Western blotting - For each clone of HEK-293F transfectants, 3X10⁶ cells were washed in PBS and extracted in RIPA buffer (50 mM Tris-HCl pH 7.4, 1% (v/v) NP40, 0.25% (w/v) sodium deoxycholate in the presence of protease inhibitors). Protein extracts were resolved on 10% SDS-PAGE [11] and transferred to PVDF membranes [12]. Membranes were probed for PfCRT expression using rabbit anti-serum raised against PfCRT N-terminal sequence (1-58 polypeptide) at 1:6000 (v/v) dilution (Baakdah F. and Georges E., unpublished results). All PVDF membranes were probed with anti-tubulin monoclonal antibody (1 µg/ml) for equal protein loading. Following overnight incubation at 4°C with primary antibodies, PVDF membranes were washed with PBS and incubated with horse radish peroxidase (HRP)-conjugated secondary antibodies (1:3000 (v/v)) diluted in 3% (w/v) milk/PBS. Membranes were washed with PBS and developed using Thermo Scientific™ SuperSignal™ West Pico

Chemiluminescent Substrate. Images were captured with ChemiDoc imaging system from BIO-RAD Inc.

Indirect immunofluorescence assay - Cells were cultivated in tissue culture onto poly L-lysine coated cover slips. The cover slips containing cells were fixed with 4% paraformaldehyde-PBS (Electron microscopy sciences) for 30 minutes at room temperature (RT). Fixed cells were washed once in PBS then quenched with 0.15% (w/v) glycine-PBS for 10 minutes at RT. Cells were washed and permeabilized with 0.1% (v/v) TritonX-100/PBS (Bio Basic Inc.) for 10 minutes at RT. Permeabilized cells were washed three times with PBS and blocked with 1% (v/v) goat serum in PBS for 1hr at 4°C. Cells were incubated with PfCRT antiserum and/or anti-sirtuin1 or anti-LAMP1 monoclonal antibodies (DSHB, at the University of Iowa, Department of Biology, USA) at 4°C overnight followed by PBS wash and probing with secondary antibody Alexa-fluor 594-conjugated goat anti-rabbit (Life Technologies™) for anti-PfCRT and Alexa-fluor 488-conjugated goat anti-mouse for the primary antibodies for 45min. The cover slips were washed three times in PBS, dipped once in distilled water, air dried and mounted on microscope slides using fluor mount G mounting medium (Southern Biotech). Images were captured using confocal microscopy (Carl Zeiss GmbH, Jena, Germany).

Dye accumulation assay - Cells were detached using 0.25% (w/v) trypsin in 0.5mM (w/v) EDTA solution. A total of 3×10^6 cells, in two sets for each cell line, were washed in HEPES-Hanks Balanced Salt Solution (HBSS) buffer (20mM (w/v) HEPES, pH 7.2 and 1 X HBSS), filter sterilized and preheated at 37°C. One set was re-suspended in 1ml of 30mM NH_4Cl HHBS buffer pH 7.2, while the second set was re-suspended in 1ml HHBS, and placed for 30minutes at 37°C. The two dyes (acridine orange (AO), Invitrogen™) or CytiPainter LysoOrange (LO) Indicator reagent, abcam®) were added to cells (4μM for AO and 2units/ml for LO) and

incubated for one hour at 37°C. After centrifugation, the resulting cell pellets of set 1 were re-suspended in 10ml 30mM NH₄Cl/HHBS buffer and set 2 were re-suspended in 10ml HHBS buffer for 1hr at 37°C. The final cell pellets were re-suspended in 1ml wash buffer and aliquoted into a round bottom black 96 well plate. Florescence was measured using Synergy H4 hybrid spectrophotometer from BioTek® and Gen5™ microplate reader and image software, according to each dye respective wavelength (AO E_x 485/E_m 530 and LO E_x 542/E_m 565). The results for dye accumulation values were adjusted for PfCRT expression and equal loading based on tubulin levels minus dye accumulation in vector transfected HEK-293F cells.

Homology Modeling - The SWISS-MODEL tool [13] was used to generate the PDB file for mut-P165A-PfCRT^{ETSE} using model-template PDB 6ukj [14] and the homology models were built and edited in PyMOL Molecular Graphics System, Version 2.0 Schrödinger, LLC.

Statistical analysis - Plotted results were analysed by one way ANOVA using GraphPad Prism version 8.4.0 (671).

RESULTS AND DISCUSSION

PfCRT-mediated drug transport studies in *P. falciparum* have been hampered by the complexity of measuring meaningful drug transport across several membranes in infected erythrocytes [15]. Hence, efforts to establish a simple *in-situ* heterologous expression system for PfCRT in HEK-293F cells stably expressing wild-type and mutant forms of PfCRT would greatly facilitate PfCRT structure-functions studies. Figure 1A shows a schematic of PfCRT secondary structure with 10 transmembrane domains and the positions of amino acid residues mapped onto the wild-type PfCRT (encoding N⁷⁵, K⁷⁶, A²²⁰ & Q²¹⁷ or wt-PfCRT^{NKAQ}), mutant-PfCRT encoding four mutations shown previously to be sufficient to confer resistance to CQ (N75E, K76T, A220S & Q217E; or mut-PfCRT^{ETSE}; [16]) and mutant-PfCRT^{ETSE} containing an additional proline to alanine mutation at position 165 (mut-P165A-PfCRT^{ETSE}). Human codon optimized full-length constructs of wt- PfCRT^{NKAQ}, mut-PfCRT^{ETSE} or mut-P165A-PfCRT^{ETSE} were linearized and transfected into HEK-293F cells. Cells were selected with 800µg/ml G418, and isolated clones were allowed to proliferate and extracted for protein analyses. Figure 1B shows Western blot results of HEK-293F extracts from cells transfected with vector alone (Vc1), vector containing wt-PfCRT^{NKAQ} (clones C2 and C4), mut-PfCRT^{ETSE} (clones C8 and C9) and mut-P165A-PfCRT^{ETSE} then probed with PfCRT N-terminal-specific antibody (PfCRT antiserum). The results in lanes 2-5 of figure 1B show a 42kDa polypeptide encoding wt-PfCRT^{NKAQ}, mut-PfCRT^{ETSE} and mut-P165A-PfCRT^{ETSE} expressed to varying levels. Interestingly, and consistently, total protein extracts from mut-PfCRT^{ETSE} clones expressed significantly less PfCRT protein than extracts from wt-PfCRT^{NKAQ} transfectants (Fig. 1B, lanes 2-3 versus 4-5). Moreover, the mut-P165A-PfCRT^{ETSE} polypeptide consistently migrated slightly faster on SDS-

PAGE than wt-PfCRT^{NKAQ} or mut-PfCRT^{ETSE} (Fig. 1B, lanes 2-5 versus 6). In addition, lanes 2, 3 and 6 revealed additional polypeptides migrating

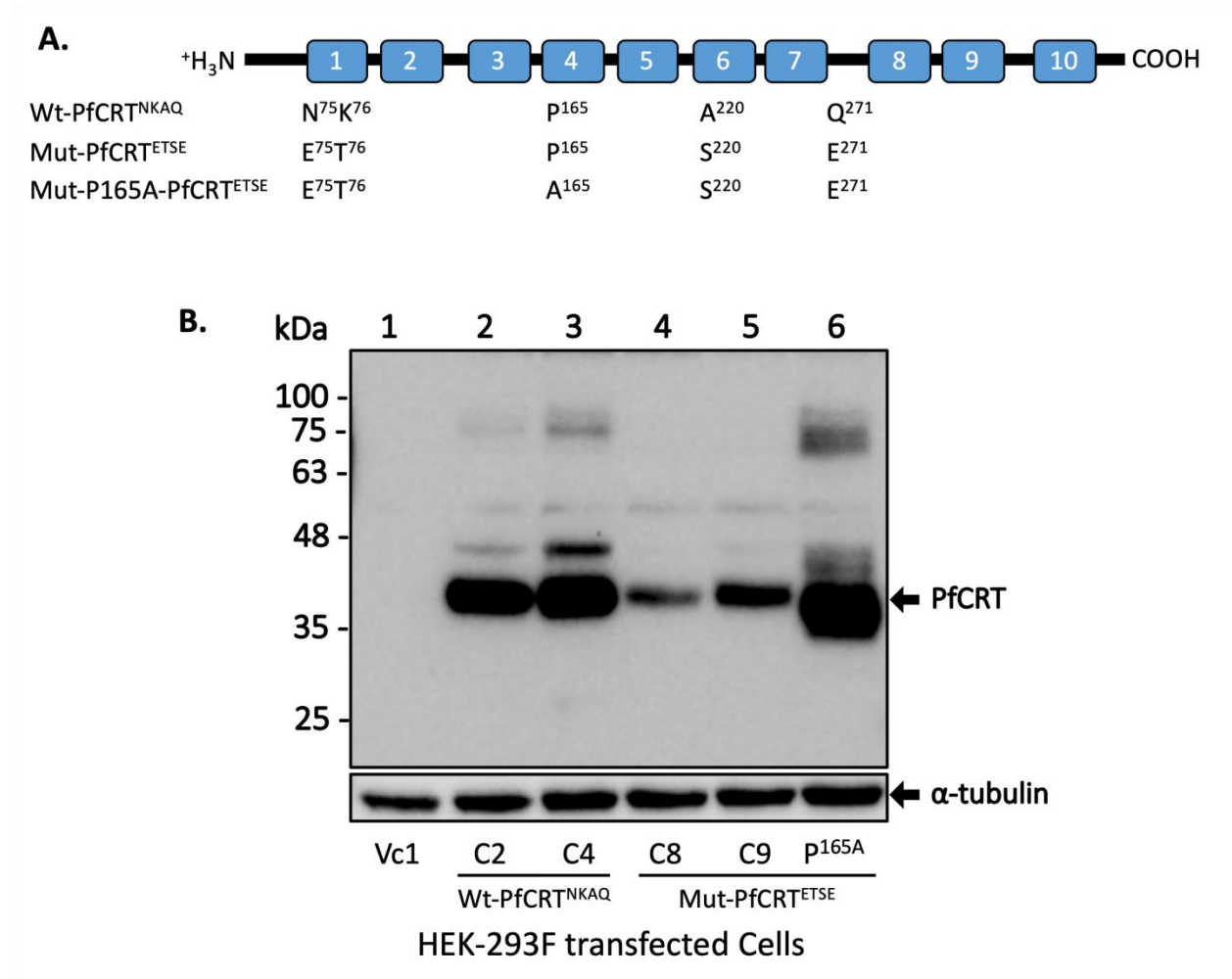


Figure 1. Stable expression of wild-type and mutant-PfCRT in HEK-293F cells. Panel A shows a schematic representation of full-length PfCRT as a solid bar with transmembrane domains indicated as blue filled rectangles (1-10). The positions of various amino acid residues found in wild-type 3D7 PfCRT (wt-PfCRT^{NKAQ}), mutant-PfCRT (mut-PfCRT^{ETSE}) and Pro165Ala substituted mutant-PfCRT^{ETSE} (mut-P165A-PfCRT^{ETSE}) are localized onto PfCRT schematic using single letter code. Panel B shows cell lysates from HEK-293F cells transfected with vector alone (Vc1; lane 1), vector containing wt-PfCRT^{NKAQ} (clones C2 and C4; lanes 2 and 3), mut-PfCRT^{ETSE} (clones C8 and C9; lanes 4 and 5) and mut-P165A-PfCRT^{ETSE} (lane 6) were resolved on 10% SDS-PAGE, transferred to PVDF membrane, and probed with PfCRT antiserum and

tubulin monoclonal antibody. PfCRT polypeptide migrated with an apparent molecular mass of 42kDa seen in all HEK-293F transfectants (lanes 2-6), except in vector transfected HEK-293F (Vc1; lane 1). The tubulin polypeptide band, loading control, is detected in all samples (lanes 1-6).

with molecular masses of ~52kDa and ~90kDa with varying intensities proportionate to the intensity of the 42kDa band suggesting that they may represent a post-translationally modified PfCRT (e.g., 52kDa) or a PfCRT homodimer (e.g., 90kDa) [17]. The latter speculations are strengthened further **since** both the 52kDa and 90kDa polypeptides in lanes 2 and 3 (wt-PfCRT^{NKAQ}) appear to migrate slightly faster in lane 6 (mut-P165A-PfCRT^{ETSE}) mimicking the slight increase in mobility of the 42kDa polypeptide. The significance of the 52kDa and 90kDa PfCRT proteins is presently not clear but appears to be present at lower levels than the 42kDa form of PfCRT.

Previous heterologous expression of wild-type HB3 and Dd2 mutant-*pfCRT* alleles into HEK-293 cells showed lysosomal localization, an equivalent organelle to the DV in *P. falciparum* [18]. To determine the subcellular localization of PfCRT in HEK-293F cells stably expressing wt-PfCRT^{NKAQ} and mut-PfCRT^{ETSE}, cells were subjected to double immunofluorescence staining (IFA) with anti-PfCRT and anti-LAMP1 (established lysosomal protein [19]) or anti-sirtuin 1 (a nuclear protein [20]) antibodies, respectively. Figure 2 shows punctate staining with anti-PfCRT and anti-LAMP1 in the cytosol and outside the cell nuclei that perfectly overlap. By contrast, and as expected, anti-sirtuin 1 stained cell nuclei and did not overlap with anti-PfCRT staining (Fig. 2). Similar results were observed for mut-PfCRT^{ETSE} and mut-P165A-PfCRT^{ETSE} (not shown). It is interesting that, unlike in HEK-293F and *P. falciparum*, PfCRT expressed in yeast and *Xenopus laevis* oocytes was shown to localize to the plasma membrane [21]. Differences in PfCRT subcellular localization between yeast and *Xenopus laevis* oocytes versus *P. falciparum*

and HEK-293F cells is not entirely clear but may be due to differential post-translational modification. With respect to the latter, it has been suggested that phosphorylation at threonine 416 in PfCRT C-terminal mediates its sorting to the DV membrane in *P. falciparum* [22]. Hence, it will be of interest to determine if PfCRT is post-translationally modified HEK-293 cells and if mutations of such post-translationally modified sites alter its subcellular localization. Given earlier findings [23] relating to increased lysosomal acidification in HEK-293 cells transiently expressing mutant Dd2-associated *pfcr*t allele, we made use of two lysosome fluorescent dyes (*i.e.*, AO and LO) to validate this function of mutant-PfCRT using HEK-293F transfectants stably expression PfCRT [24].

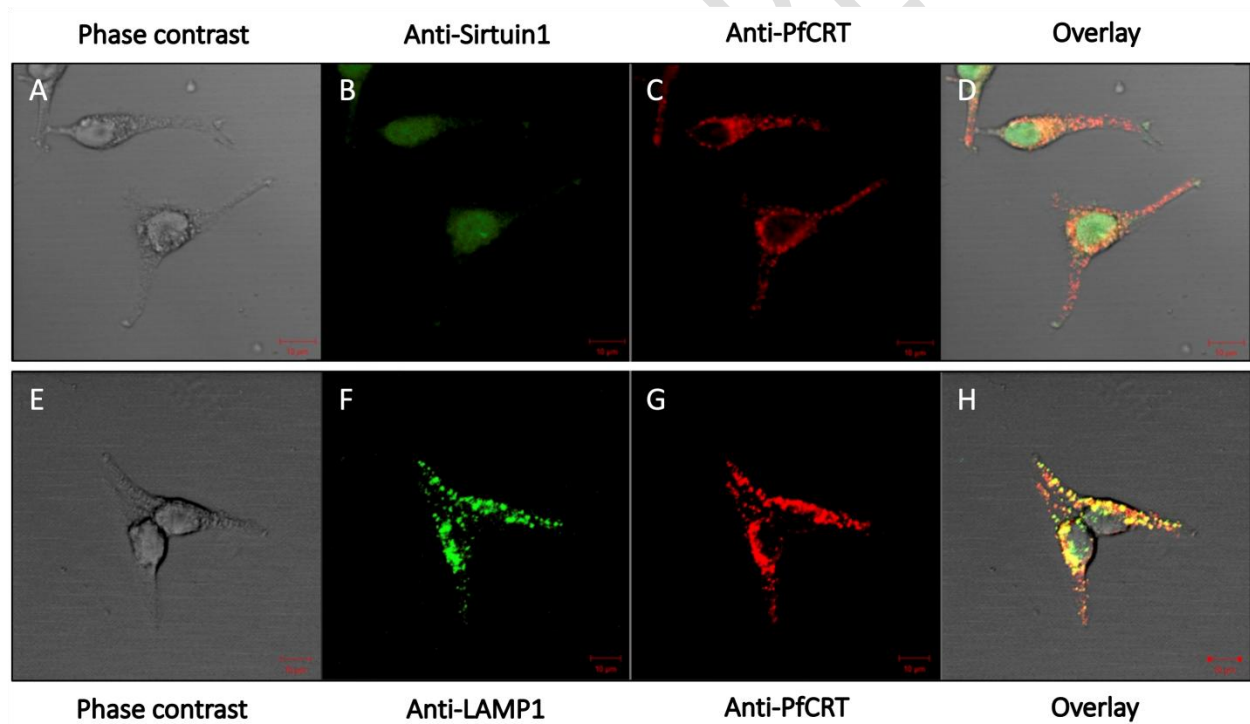


Figure 2. Immuno-fluorescence staining of PfCRT in HEK-293F cells. PfCRT-HEK clones were prepared for IFA and images were taken using confocal microscopy. Panels C and G show cells expressing wt-PfCRT^{NKAQ} when stained with PfCRT antisera; while Panels B and F show cells stained with anti-sirtuin1 or anti-LAMP1, respectively. Panels D and H show the overlay of Panels B+C and D+G, respectively. Panels A and E show the phase contrast images of cells expressing wt-PfCRT^{NKAQ}. The scale bar on each panel reads 10μm.

The results in figure 2A shows the relative accumulation of AO in HEK-293F cells stably transfected with wt-PfCRT^{NKAQ} (clones C2 and C4) and mut-PfCRT^{ETSE} (clones C8 and C9) relative to vector transfected cells adjusted to PfCRT protein expression levels. The results of figure 2A show dramatic increase in AO accumulation in clones C8 and C9 expressing mut-PfCRT^{ETSE} relative to clones C2 and C4 which express wt-PfCRT^{NKAQ}. This increased AO accumulation seen in clones C8 and C9 is likely due to the enhanced acidification of the lysosomal vesicles by mut-PfCRT^{ETSE} (Fig. 2A). Moreover, short-term pre-incubation of cells expressing both wt-PfCRT^{NKAQ} and mut-PfCRT^{ETSE} in 30mM NH₄Cl completely abolished the accumulation of AO in all cells relative to vector transfected HEK-293F cells, confirming the role of differential proton gradient on AO accumulation (Fig. 2A). Similar results were seen using a different lysosome targeting dye, LO (Fig. 2B), confirming the effect of mut-PfCRT^{ETSE} on the acidification of lysosomes in HEK-293F cells (clones C8 and C9), relative to wt-PfCRT^{NKAQ} expressing clones (C2 and C4). The mutations in PfCRT selected in this study (*i.e.*, mut-PfCRT^{ETSE}) were the same mutations that increased the uptake of CQ in *Xenopus laevis* oocytes, but are three fewer mutations than Dd2-PfCRT [25] used in an earlier study to demonstrate lysosomal acidification in HEK-293 cells [26]. Hence, we speculate that there may be a correlation between PfCRT ability to transport CQ into *Xenopus laevis* oocytes (which is consistent with CQ resistance based on PfCRT's orientation in the DV membrane) and lysosome acidification in HEK-293 cells [27]. The latter speculation is supported by earlier observation in *Dictyostelium discoideum*, whereby mutant-PfCRT expelled CQ and caused a significant intravesicular acidification of the acidic vesicles [28]. Moreover, it was previously shown that mutant alleles of *pfert* from CQR strains (e.g., 7G8 and Dd2) conferred increased acidification of the DV relative to CQS strains [24].

To confirm the direct role of mut-PfCRT in lysosomal acidification in HEK-293 cells and to determine the effects of specific amino acids substitutions on PfCRT segregate function in HEK-293F cells (*i.e.*, lysosomal acidification), it was of interest to examine the effects of substituting two proline residues (Pro165 and Pro354) on mut-PfCRT function.

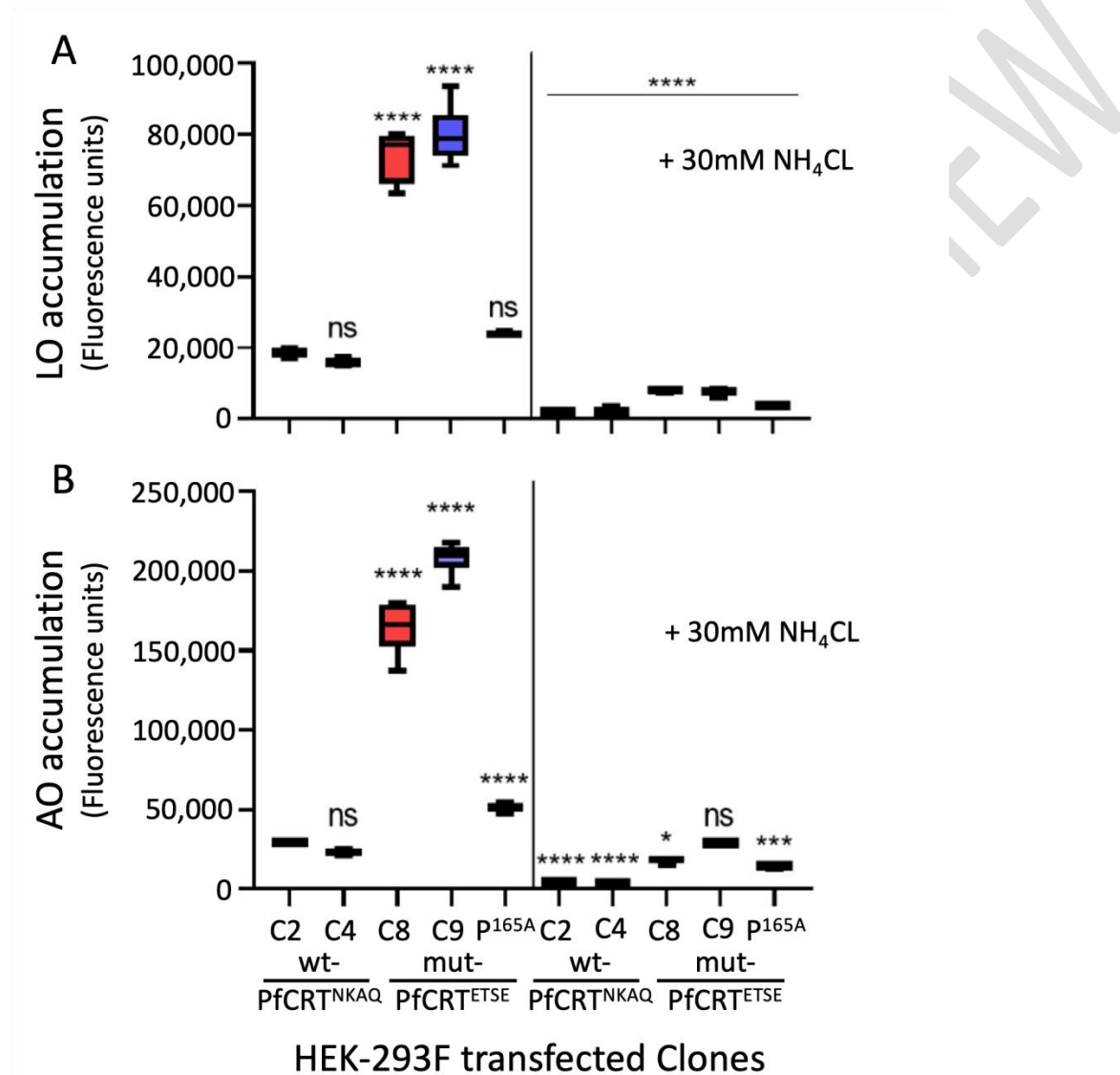


Figure 3. Accumulation of AO and LO in HEK-293F cells stably expressing wild-type and mutant-PfCRT. HEK-293F cells stably expressing wt-PfCRT^{NKAQ} (clones C2 and C4), mut-PfCRT^{ETSE} (clones C8 and C9) and mut-P165A-PfCRT^{ETSE} were incubated with AO (Panel A) or LO (Panel B) without and with 30mM NH₄Cl, respectively. The relative accumulation of AO

and LO, in arbitrary fluorescence units, is shown on the Y-axis. Results represent experiments from three independent repeats done in triplicates. Statistical significance (**** P value <0.0001) was analysed by one way ANOVA using GraphPad Prism.

The rationale for selecting Pro¹⁶⁵ and Pro³⁵⁴ was based on several points: a) both residues are highly conserved in *Plasmodium* orthologues of PfCRT, b) their localization in TM helices 4 and 9 is likely to affect helical distortion and flexibility of these domains, and c) proline residues in α -helical TMDs play structural and/or functional roles in polytopic membrane proteins whereby the geometry and the limited hydrogen bonding of this residue introduce a molecular joint or hinge that could be important for function [29]. Therefore, proline residues in TM helices can have important structural and/or functional roles in membrane proteins. Moreover, substitution of proline by alanine, an amino acid with the highest helix propensity, contrary to proline, should have minimal effects on PfCRT structural integrity and would eliminate the possible molecular hinge introduced by proline [28]. The results in figure 3A and 3B show the effect of Pro165Ala on AO and LO accumulation in HEK-293 cells expressing mut-P165A-PfCRT^{ETSE}. The substitution of Pro165 for Ala-165 in TMD4 of mut-PfCRT^{ETSE} completely abolished its lysosome acidification function to the same level as wt-PfCRT^{NKAQ} as measured by the accumulation of AO and LO in HEK-293F cells (Fig. 3A and 3B, respectively). Furthermore, treatment of cells with NH₄Cl caused further decrease in AO and LO accumulation, relative to control vector transfected HEK-293F cells (Fig. 3A and 3B, respectively). It is interesting to note that unlike mut-PfCRT^{ETES} HEK-293F transfectants, both Pro165Ala-PfCRT^{ETES} and wt-PfCRT^{NKAQ} HEK-293F transfectants expressed higher levels of PfCRT which could be related to their inability to function as lysosomal acidifiers and as such higher expression levels are tolerated. Although it is not entirely clear how substituting Pro165 for Ala inhibits mut-PfCRT^{ETSE} ability to acidify the lysosomes, it has been suggested that residues in TMD 4 and 9

may contribute to the “*open and close*” conformations at the vacuolar side of the DV, while residues in TMD 5 and 10 may play the same role on the opposite side of the membrane in a “*rocker-switch*” movement [9]. Based on the resolved structure of 7G8 mutant-PfCRT [30], Pro165 is localized midway in TM helix 4 facing outside the central cavity formed by TMDs 1-4 and 6-9, but in close contact with TM helix 5 (Fig. 4). In support of the latter speculation, figure 4 shows a slight shift TM4 helix with Ala165 versus Pro165 which may affect PfCRT proposed “*rocker-switch*” movement and consequently its function. Similarly, P354 is also localized roughly midway of TM helix 9 facing outside pore cavity, and in close vicinity of TMD 10 (Fig. 4).

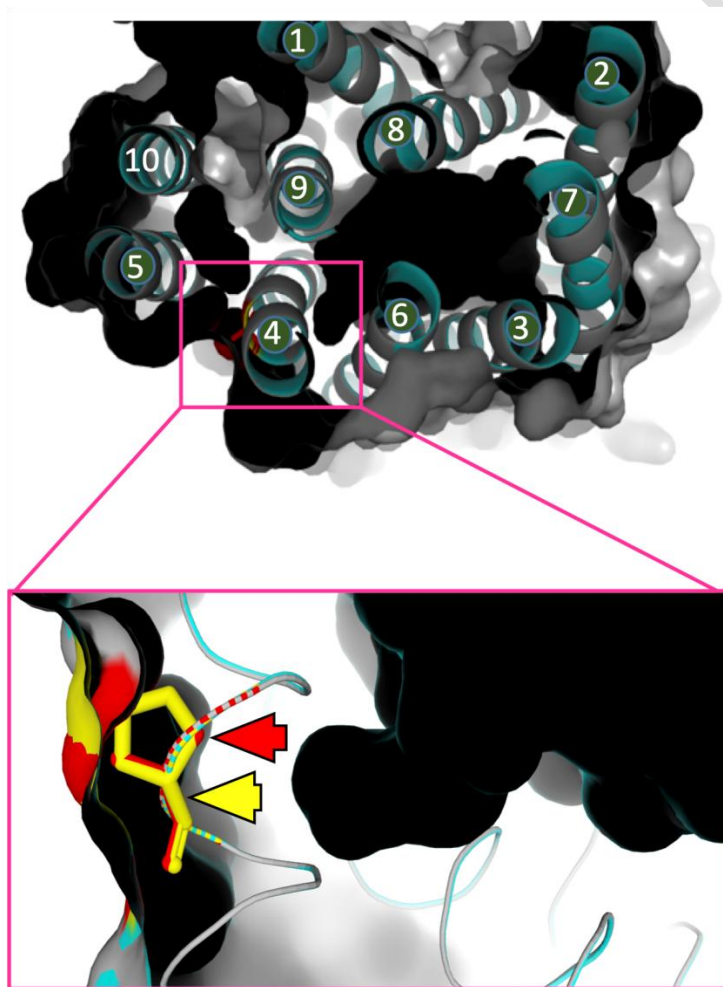


Figure 4. PfCRT homology modeling with P-165-A substitution in mut-PfCRT. The homology modeling of PfCRT was done based on PfCRT-7G8-Pro165 TMD's crystal structure (PDB 6UKJ). In blue are the TMDs of mut-PfCRT-7G8 overlapping with the gray TMDs of mut-P165A-PfCRT^{ETSE}. In yellow is the proline (yellow arrow) and in red is the alanine (red arrow).

Together, it is likely that TMD 4 and 9 modulate PfCRT transport function through their interactions with TMD 5 and 10. Unfortunately it was not possible to test the effect of Pro-365 substitution on PfCRT function. Moreover, it would be of interest to test the role of Pro165 substitution on the ability of mutant-PfCRT to confer resistance to CQ in the parasite. Given that PfCRT is likely to continue performing its normal function in CQ-resistant strains, it would be equally important to test if substituting Pro165 with Ala affects both the wt-type and mutant-PfCRT functions in the parasite's DV.

PfCRT is a member of the drug/metabolite transporter superfamily and may act as a proton-coupled transporter as other members of the family [31]. However, it was reported that parasite strains encoding CQ-resistant mutants of PfCRT allow leakage of protons from the DV [32]. The latter results are at odds with our findings and those by Reeves *et al.* [16]. However, it is likely that in HEK-293 cells, mut-PfCRT^{ETSE} does not transport the same substrate in the parasite DV. Moreover, mut-PfCRT^{ETSE} in HEK-293F does not seem to mediate the efflux of CQ from lysosomes (results not shown and [16]) and consequently, proton-leakage from the parasite DV appears to be associated with CQ-efflux. We speculate that mut-PfCRT^{ETSE} expressed in HEK-293F may not undergo similar post-translational modification to that in *P. falciparum* and this could affect its CQ-mediated drug resistance and transport functions. In line with the latter possibility, a recent report demonstrating a 50% reduction in CQ resistance following the substitution of Ser33 to Ala, but not Asp phospho-mimic, in Dd2 *P. falciparum* isolate [30].

Conclusion – The results of this study describe the use of HEK-293F human cell line stably expressing a heterologous malaria membrane protein that localize to the lysosomal membrane, an equivalent organelle to the digestive vacuole in *P. falciparum*, hence establishing PfCRT-HEK-293F cells as a heterologous expression system to study PfCRT structure-function. Moreover, consistent with earlier study, we demonstrate the ability of mutant PfCRT (mut-PfCRT^{ETSE}, a chloroquine competent transporter) can cause the acidification of lysosomes in HEK-293F cells. Lastly, we show for the first time that mutations of certain amino acids (e.g., Pro165 to Ala) in transmembrane 4 of PfCRT abolishes the ability of mut-P165A-PfCRT^{ETSE} to acidify the lysosomal compartment in HEK-293F cells. Work in progress is focused on establishing HEK-293F cells stably expressing wild-type and mutant PfCRT as a segregate system to study the mechanism of PfCRT mediated CQ-resistance.

COMPETING INTERESTS DISCLAIMER:

Authors have declared that no competing interests exist. The products used for this research are commonly and predominantly use products in our area of research and country. There is absolutely no conflict of interest between the authors and producers of the products because we do not intend to use these products as an avenue for any litigation but for the advancement of knowledge. This work was supported by funds from the Natural Sciences and Engineering Research Council of Canada (EG) and King Abdulaziz University (FB).

REFERENCE LIST

1. Organization. GWH. World Malaria Report. World Health Organization [WHO]. 2019;ISBN: 978-92-4-156572-1.
2. Jensen M, Mehlhorn H. Seventy-five years of Resochin in the fight against malaria. *Parasitology research*. 2009;105(3):609-27; doi: 10.1007/s00436-009-1524-8.
3. Fidock DA, Nomura T, Talley AK, Cooper RA, Dzekunov SM, Ferdig MT, et al. Mutations in the *P. falciparum* digestive vacuole transmembrane protein PfCRT and evidence for their role in chloroquine resistance. *Molecular cell*. 2000;6(4):861-71; doi: 10.1016/s1097-2765(05)00077-8.
4. Summers RL, Dave A, Dolstra TJ, Bellanca S, Marchetti RV, Nash MN, et al. Diverse mutational pathways converge on saturable chloroquine transport via the malaria parasite's chloroquine resistance transporter. *Proceedings of the National Academy of Sciences of the United States of America*. 2014;111(17):E1759-67; doi: 10.1073/pnas.1322965111.
5. Johnson DJ, Fidock DA, Mungthin M, Lakshmanan V, Sidhu AB, Bray PG, et al. Evidence for a central role for PfCRT in conferring *Plasmodium falciparum* resistance to diverse antimalarial agents. *Molecular cell*. 2004;15(6):867-77; doi: 10.1016/j.molcel.2004.09.012.
6. Martin RE, Kirk K. The malaria parasite's chloroquine resistance transporter is a member of the drug/metabolite transporter superfamily. *Molecular biology and evolution*. 2004;21(10):1938-49; doi: 10.1093/molbev/msh205.

7. Kim J, Tan YZ, Wicht KJ, Erramilli SK, Dhingra SK, Okombo J, et al. Structure and drug resistance of the Plasmodium falciparum transporter PfCRT. *Nature*. 2019;576(7786):315-20; doi: 10.1038/s41586-019-1795-x.
8. Waller KL, Muhle RA, Ursos LM, Horrocks P, Verdier-Pinard D, Sidhu AB, et al. Chloroquine resistance modulated in vitro by expression levels of the Plasmodium falciparum chloroquine resistance transporter. *The Journal of biological chemistry*. 2003;278(35):33593-601; doi: 10.1074/jbc.M302215200.
9. Coppee R, Sabbagh A, Clain J. Structural and evolutionary analyses of the Plasmodium falciparum chloroquine resistance transporter. *Scientific reports*. 2020;10(1):4842; doi: 10.1038/s41598-020-61181-1.
10. Gibson DG. Enzymatic assembly of overlapping DNA fragments. *Methods in enzymology*. 2011;498:349-61; doi: 10.1016/b978-0-12-385120-8.00015-2.
11. Laemmli UK. Cleavage of structural proteins during the assembly of the head of bacteriophage T4. *Nature*. 1970;227(5259):680-5; doi: 10.1038/227680a0.
12. Towbin H, Staehelin T, Gordon J. Electrophoretic transfer of proteins from polyacrylamide gels to nitrocellulose sheets: procedure and some applications. *Proceedings of the National Academy of Sciences of the United States of America*. 1979;76(9):4350-4.
13. Waterhouse A, Bertoni M, Bienert S, Studer G, Tauriello G, Gumienny R, et al. SWISS-MODEL: homology modelling of protein structures and complexes. *Nucleic acids research*. 2018;46(W1):W296-w303; doi: 10.1093/nar/gky427.
14. Jackson KE, Klonis N, Ferguson DJ, Adisa A, Dogovski C, Tilley L. Food vacuole-associated lipid bodies and heterogeneous lipid environments in the malaria parasite,

- Plasmodium falciparum*. *Molecular microbiology*. 2004;54(1):109-22; doi: 10.1111/j.1365-2958.2004.04284.x.
15. Kell DB, Oliver SG. How drugs get into cells: tested and testable predictions to help discriminate between transporter-mediated uptake and lipoidal bilayer diffusion. *Frontiers in pharmacology*. 2014;5:231; doi: 10.3389/fphar.2014.00231.
 16. Reeves DC, Liebelt DA, Lakshmanan V, Roepe PD, Fidock DA, Akabas MH. Chloroquine-resistant isoforms of the *Plasmodium falciparum* chloroquine resistance transporter acidify lysosomal pH in HEK293 cells more than chloroquine-sensitive isoforms. *Molecular and biochemical parasitology*. 2006;150(2):288-99; doi: 10.1016/j.molbiopara.2006.09.001.
 17. Meikle PJ, Brooks DA, Ravenscroft EM, Yan M, Williams RE, Jaunzems AE, et al. Diagnosis of lysosomal storage disorders: evaluation of lysosome-associated membrane protein LAMP-1 as a diagnostic marker. *Clinical chemistry*. 1997;43(8 Pt 1):1325-35.
 18. Sun L, Fang J. Macromolecular crowding effect is critical for maintaining SIRT1's nuclear localization in cancer cells. *Cell cycle*. 2016;15(19):2647-55; doi: 10.1080/15384101.2016.1211214.
 19. Zhang H, Howard EM, Roepe PD. Analysis of the antimalarial drug resistance protein PfCRT expressed in yeast. *The Journal of biological chemistry*. 2002;277(51):49767-75; doi: 10.1074/jbc.M204005200.
 20. Nessler S, Friedrich O, Bakouh N, Fink RH, Sanchez CP, Planelles G, et al. Evidence for activation of endogenous transporters in *Xenopus laevis* oocytes expressing the *Plasmodium falciparum* chloroquine resistance transporter, PfCRT. *The Journal of biological chemistry*. 2004;279(38):39438-46; doi: 10.1074/jbc.M404671200.

21. Kuhn Y, Sanchez CP, Ayoub D, Saridaki T, van Dorsselaer A, Lanzer M. Trafficking of the phosphoprotein PfCRT to the digestive vacuolar membrane in *Plasmodium falciparum*. *Traffic* (Copenhagen, Denmark). 2010;11(2):236-49; doi: 10.1111/j.1600-0854.2009.01018.x.
22. Tanaka Y, Suzuki G, Matsuwaki T, Hosokawa M, Serrano G, Beach TG, et al. Progranulin regulates lysosomal function and biogenesis through acidification of lysosomes. *Human molecular genetics*. 2017;26(5):969-88; doi: 10.1093/hmg/ddx011.
23. Naude B, Brzostowski JA, Kimmel AR, Welles TE. Dictyostelium discoideum expresses a malaria chloroquine resistance mechanism upon transfection with mutant, but not wild-type, *Plasmodium falciparum* transporter PfCRT. *The Journal of biological chemistry*. 2005;280(27):25596-603; doi: 10.1074/jbc.M503227200.
24. Bennett TN, Kosar AD, Ursos LMB, Dzekunov S, Singh Sidhu AB, Fidock DA, et al. Drug resistance-associated pfCRT mutations confer decreased *Plasmodium falciparum* digestive vacuolar pH. *Molecular and biochemical parasitology*. 2004;133(1):99-114; doi: <https://doi.org/10.1016/j.molbiopara.2003.09.008>.
25. Williams KA, Deber CM. Proline residues in transmembrane helices: structural or dynamic role? *Biochemistry*. 1991;30(37):8919-23; doi: 10.1021/bi00101a001.
26. Cordes FS, Bright JN, Sansom MS. Proline-induced distortions of transmembrane helices. *Journal of molecular biology*. 2002;323(5):951-60; doi: 10.1016/s0022-2836(02)01006-9.
27. Kim MK, Kang YK. Positional preference of proline in alpha-helices. *Protein science : a publication of the Protein Society*. 1999;8(7):1492-9; doi: 10.1110/ps.8.7.1492.

28. Pace CN, Scholtz JM. A helix propensity scale based on experimental studies of peptides and proteins. *Biophysical journal*. 1998;75(1):422-7; doi: 10.1016/s0006-3495(98)77529-0.
29. Lehane AM, Kirk K. Chloroquine resistance-conferring mutations in pfert give rise to a chloroquine-associated H⁺ leak from the malaria parasite's digestive vacuole. *Antimicrobial agents and chemotherapy*. 2008;52(12):4374-80; doi: 10.1128/aac.00666-08.
30. Sanchez CP, Moliner Cubel S, Nyboer B, Jankowska-Dollken M, Schaeffer-Reiss C, Ayoub D, et al. Phosphomimetic substitution at Ser-33 of the chloroquine resistance transporter PfCRT reconstitutes drug responses in *Plasmodium falciparum*. *The Journal of biological chemistry*. 2019;294(34):12766-78; doi: 10.1074/jbc.RA119.009464.
31. Antony HA, Topno NS, Gummadi SN, Siva Sankar D, Krishna R, Parija SC. In silico modeling of *Plasmodium falciparum* chloroquine resistance transporter protein and biochemical studies suggest its key contribution to chloroquine resistance. *Acta Trop*. 2019;189:84-93; doi: 10.1016/j.actatropica.2018.10.001.
32. Shafik SH, Cobbold SA, Barkat K, Richards SN, Lancaster NS, Llinás M, et al. The natural function of the malaria parasite's chloroquine resistance transporter. *Nat Commun*. 2020;11(1):3922; doi: 10.1038/s41467-020-17781-6.